International Journal of Hydrogen Energy 142 (2025) 122–129

Contents lists available at ScienceDirect

International Journal of Hydrogen Energy

journal homepage: www.elsevier.com/locate/he

Developed empirical correlation for self-pressurization in multi-configuration non-venting liquid hydrogen tanks using trust-region reflective algorithm

Anas A. Rahman [a,b,c,*], Bo Wang [a,**], Jingshan Yan [d], Haoren Wang [a,b], Tao Jin [b], Zhihua Gan [a,b]

[a] *Cryogenic Center, Hangzhou City University, Hangzhou, 310015, China*
[b] *Key Laboratory of Refrigeration and Cryogenic Technology of Zhejiang Province, Zhejiang University, Hangzhou, 310027, China*
[c] *Department of Mechanical Engineering, Future University in Egypt, End of 90th St., Fifth Settlement, New Cairo, Cairo, 11835, Egypt*
[d] *School of Information Science and Engineering, Shandong University, Qingdao, Shandong, 266237, China*

ARTICLE INFO

Keywords:
Developed empirical correlation
Trust-region reflective algorithm
Non-venting liquid hydrogen tank
Self-pressurization
Pressurization rate
Multi-configuration liquid hydrogen tanks

ABSTRACT

Liquid hydrogen (LH_2) has emerged as a promising solution for decarbonization and global warming mitigation, offering high volumetric energy density, low-operating pressure, and environmental friendliness. A key challenge in non-venting LH_2 tanks is accurately predicting the self-pressurization rate, requiring complex thermal models which are computationally expensive and time-consuming. Conversely, empirical correlations can simplify the modeling process and aid in the design of LH_2 tanks for safe storage, transportation, and utilization without venting risks. This study presents an empirical correlation for self-pressurization in multi-configuration LH_2 tanks, developed using published experimental data and the trust-region reflective algorithm. The developed correlation improves upon existing correlations, providing robust, reliable and consistent predictions. Compared to experimental results, the correlation achieves an acceptable prediction error margin of $\pm$ 10%, with an average error of 1.49 %. The findings offer valuable insights for the design and optimization of LH_2 tanks.

1. Introduction

Nowadays, the demand for liquid hydrogen (LH_2) as a promising energy carrier is rapidly increasing due to its advantages over conventional fuels, including higher energy density, sustainability, and environmental benefits [1]. However, safe storage, transportation, and utilization of LH_2 present significant challenges due to the self-pressurization phenomenon. This occurs when heat leakage from the surroundings leads to pressure buildup, accompanied by other thermal effects such as thermal stratification, liquid thermal expansion, and the interfacial evaporation/condensation process [2,3]. As the vapor pressure inside the LH_2 tank exceeds the maximum allowable working pressure, boil-off gas (BOG) is vented to the atmosphere. As well-known, LH_2 is highly flammable and any venting or leaks of hydrogen gas pose a significant explosion risk, with potentially severe environmental consequences [1]. Therefore, accurately predicting pressure changes in non-venting, self-pressurized LH_2 tanks is crucial to ensure pressure stability and mitigate venting risks.

A review of the literature reveals that numerous experimental, theoretical, numerical and empirical studies were conducted to analyze pressure evolution in LH_2 tanks [1]. Specifically, extensive experimental investigations [2] focused on identifying key parameters that influence pressure evolution, such as heat flux, initial operating pressure, initial liquid filling ratio, tank volume, and hold time. These studies [2] also examined various tank shapes and sizes, highlighting the nonlinear nature of pressure evolution under different operating conditions. Furthermore, numerous theoretical [4,5] and numerical models [1] were developed to predict pressure evolution in LH_2 tanks. However, these models showed significant deviations from experimental results.

Modeling of the self-pressurization phenomenon in LH_2 tanks still presents significant challenges, leading to the development of empirical correlations which can simplify the modeling process and aid in the design of LH_2 tanks. Such correlations directly relate LH_2 pressurization rates to design parameters, typically derived from experimental data. In

* Corresponding author. Cryogenic Center, Hangzhou City University, Hangzhou, 310015, China.
** Corresponding author.
E-mail addresses: arahman@zju.edu.cn (A.A. Rahman), wangbo@hzcu.edu.cn (B. Wang).

https://doi.org/10.1016/j.ijhydene.2025.05.393
Received 17 March 2025; Received in revised form 27 May 2025; Accepted 28 May 2025
Available online 3 June 2025

this regard, few studies focused on developing empirical correlations for pressure evolution in non-venting LH_2 tanks under varying design conditions. Notably, Blatt [6] proposed an empirical correlation relating pressurization rates to design parameters such as heat input, initial filling ratio, and tank size, based on experimental data from both ground and flight tests of LH_2 and liquid oxygen. However, this correlation exhibited significant discrepancies, mainly due to its inadequacy to account for the nonlinear nature of pressure evolution and its partial dependence on LH_2 experimental data. Further details on Blatt's empirical correlation are provided in Section S.1 in the Supplementary Materials.

In the present work, the trust-region reflective (TRR) algorithm is introduced as a promising nonlinear parametric fitting approach to address the key research gap represented in the lack of effective thermal design approaches for predicting LH_2 self-pressurization rate under varying design conditions. More specific, a closed-form analytical formula was developed as an empirical correlation for self-pressurization in multi-configuration LH_2 tanks, with accurately determining its empirical coefficients using the trust-region reflective (TRR) optimization algorithm.

The TRR algorithm is a promising optimization method for nonlinear least-squares parametric fitting [7,8]. The attractiveness of the TRR approach stems from its reliability, robustness, applicability to ill-conditioned problems, and strong convergence properties [7,9]. Recently, various studies have demonstrated the strong capability of the TRR algorithm in addressing complex nonlinear parametric fitting problems [8,10,11]. For instance, Wu et al. [8] combined the TRR algorithm with the artificial bee colony to significantly enhance parameter extraction for solar photovoltaic models. Similarly, Le et al. [10] utilized the TRR algorithm to accurately determine the creep model parameters of soft soil by providing a numerical solution for the nonlinear elastic-visco-plastic model. Gao et al. [11] applied the opposite normalized trust-region reflective algorithm to successfully extract parameters for single-, double-, and triple-diode solar cell models. These studies collectively demonstrate the TRR algorithm's effectiveness in developing robust empirical correlations with strong predictive capabilities. In contrast, limited research work has focused on nonlinear empirical modeling of LH_2 pressure evolution [12]. Notably, Rahman et al. [12] developed an artificial neural network (ANN)-based correlation for accurately predicting the self-pressurization rate in quasi-spherical LH_2 tanks.

In this study, an empirical correlation for self-pressurization in LH_2 tanks is developed using consolidated experimental data from three LH_2 tanks with distinct configurations: cylindrical [13], spherical [14], and elliptical [15], as given in Table S.2 in the Supplementary Materials. A detailed description of these tanks is provided in Section 2. The main findings of this work are: (i) Demonstrating the TRR algorithm as an effective approach with enhanced applicability for developing robust empirical correlations; (ii) Improving the accuracy of self-pressurization predictions compared to existing theoretical correlations; and (iii) Highlighting the potential of the TRR algorithm to address design challenges of LH_2 energy storage systems.

2. Methodology for developing the empirical correlation of LH_2 pressurization

2.1. Physical models

From a practical perspective, this study investigates three multi-configuration LH_2 tanks as the physical models, including different tank sizes, shapes and operational ranges. These three LH_2 tanks include the Multi-purpose Hydrogen Test Bed (MHTB) [13], the large spherical Dewar [14], and the K-site [15] LH_2 tank, as illustrated in Fig. 1. The geometrical dimensions of such tanks are provided in Table 1, while the variables and their operating ranges for the proposed empirical correlation are listed in Table 2.

2.2. Trust-region reflective algorithm for predicting self-pressurization in LH_2 tanks

2.2.1. Problem definition

In practical engineering, it is often necessary to fit a set of data points to parameters (i.e., coefficients) that reflect the underlying behavior of the data. To achieve this, reasonable assumptions about the data's functional form are made, incorporating external knowledge of the physical process. These assumptions help ensure that the fit is consistent with the physical principles governed by the internal variables of the system. In this study, an exponential function was chosen as the analytical form for the proposed empirical correlation, based on prior experience in modeling the relationship between vapor pressure and hold time [2] under varying initial operating pressures, heat fluxes, filling ratios, and tank volumes.

Solving nonlinear parametric fitting problems typically involves two key aspects: (i) The well-defined nonlinear nature of the problem; and (ii) The efficient handling of variable bounds. A primary focus of this study is the application of the trust-region reflective (TRR) algorithm, a

Table 1
Geometrical dimensions of the investigated LH_2 tanks.

LH_2 test facilities	*Dimensions*	*Value*
Cylindrical MHTB tank [13]	Diameter, D Height, H Elliptical dome head ratio	3.05 m 3.05 m 2:1
Large spherical Dewar [14]	Diameter, D	*7.35 m*
Elliptical K-site tank [15]	Major diameter, D_{major} Major-to-minor axis ratio	2.2 m 1.2

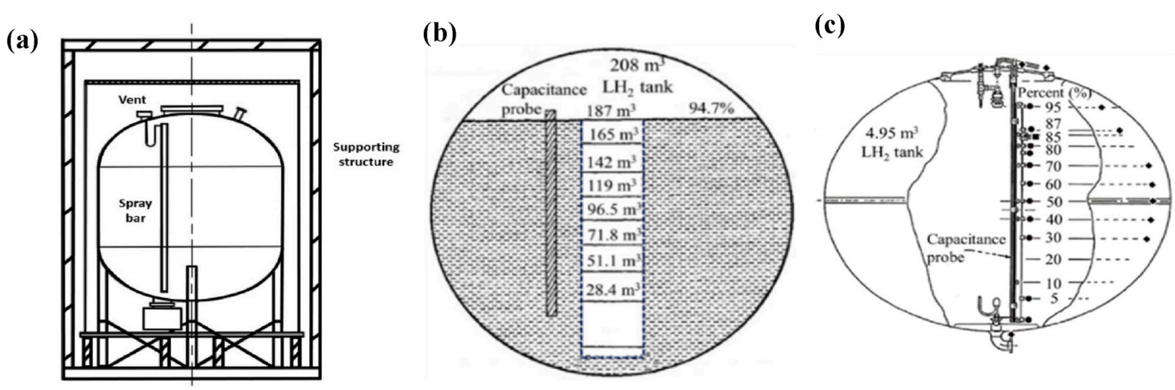

Fig. 1. Schematic sketches of multi-configuration LH_2 tanks: (a) MHTB tank [13]; (b) Large spherical Dewar [14]; and (c) K-site tank [15].

Table 2
Proposed empirical correlation variables and their operating ranges.

Variable	*Range*
Initial operating pressure (P_i) [MPa]	0.103 - 0.130244503
Tank volume (V) [m^3]	4.89 - 208
Heat flux (q) [W/m^2]	0.35 - 3.5
Initial liquid filling ratio (φ) [−]	0.25 - 0.9
Non-venting hold time (t) [hr]	0 - 38.02569458
Final vapor pressure (P_f) [MPa]	0.103 - 0.26900383

Table 3
Comparison among different parametric fitting methods under the same number of empirical coefficients.

Parameter fitting method	Average training (or fitting) error [%]	Average testing error [%]
Trust-region	1.5	1.2
Multiple linear regression	7.3	6.6
Levenberg-Marquardt	5.2	4.5
Nelder-Mead	13	12.4

class of effective numerical optimization techniques closely related to function approximation [7]. The TRR algorithm provides accurate estimates for the unknown coefficients in the proposed empirical correlation for self-pressurization in LH_2 tanks.

2.2.2. *Objective function for the empirical correlation coefficient determination*

Accurately fitting the pressure-time (*P-t*) characteristic curves for the considered LH_2 tanks is essential for estimating the empirical correlation coefficients. The unknown coefficients were optimized to minimize the deviation between the computed and experimental pressure-time curves using the TRR algorithm. To achieve this, the objective function must first be defined. The root mean square error (*RMSE*) and the sum of squared residuals (*SSR*) are commonly used metrics [8,11] to quantify the overall deviation between the computed final pressures and their corresponding experimental values at specific times. While the *RMSE* and *SSR* are comparable, with the *RMSE* directly calculated from the *SSR* [8], the SSR was chosen here due to its interpretability in measuring total error in the model's predictions. Specifically, the *SSR* quantifies how much the observed values deviate from the fitted model, providing a balanced measure of bias (systematic error) and variance (random error). The *RMSE*, on the other hand, accounts for both variance and bias, reflecting not only the magnitude of errors but also their consistency across different predictions. The expressions for *SSR* and *RMSE* are given in Eqs. (1) and (2), respectively [8,11].

$$F(X) = SSR(X) = \sum_{i=1}^{N} f\left(P^i, t^i, X\right)^2, \tag{1}$$

$$RMSE(X) = \sqrt{F(X)/N}, \tag{2}$$

where P^i denotes the observed final pressure at a given time t^i. N represents the number of measured *P-t* data points, and X represents a parameter vector with five dimensions: initial operating pressure, heat flux, initial liquid filling ratio, tank volume, and hold time, which include the unknown empirical coefficients. The fitted model parameter vector X is constrained within lower and upper bounds (*LB* and *UB*). The objective of this study is to determine the optimal parameter vector X, and hence the optimal empirical coefficients, by minimizing either the *RMSE* or *SSR*.

2.2.3. *Trust-region reflective algorithm*

The trust-region reflective (TRR) algorithm is an effective method for solving bound-constrained nonlinear minimization problems, such as nonlinear least squares data-fitting problems [16,17], as expressed in Eq. (3) [11]. This approach aligns perfectly with the objective functions given in Eqs. (1) and (2).

$$F(X) = \min_{X \in [LB, UB]} \left[f_1(X)^2 + f_2(X)^2 + \cdots + f_N(X)^2\right] \tag{3}$$

The TRR method approximates $F(X)$ with a quadratic function $q(s)$ within a small neighborhood N around the current point X, known as the trust-region [11]. By minimizing the trust-region subproblem: $min[q(s), s \in N]$, a trial step (s) is obtained, indicating the direction for reducing $F(X)$. If $F(X + s) < F(X)$, the current point X is updated to $X + s$; otherwise, X remains unchanged, and the trust-region radius (Δ) is shrunk for the next iteration [11]. The core of the TRR algorithm is solving the trust-region quadratic subproblem to guide the search for optimal coefficients within the defined trust-region [9]. The TRR algorithm was implemented on the MATLAB platform, based on the subspace trust-region method and the interior reflective Newton algorithm proposed by Coleman et al. [16,17] and Branch et al. [18]. The key steps of the TRR methodology are provided in Section S.3 in the Supplementary Materials.

In the TRR optimization algorithm, an approximate function (i.e., the proposed exponential function for empirically correlating pressurization in LH_2 tanks) is developed by setting its empirical coefficients to proper initial guesses to ensure fast convergence at each iteration [9]. These initial guesses typically require multiple trials while monitoring the corresponding sum of squared residuals (*SSR*) or root mean square error (*RMSE*). The approximate function is then iteratively updated and refined within a specific trust region. Specifically, in the first iteration, the trust region is defined, within which the approximate function is solved to determine the empirical coefficients. Subsequently, the trial step within the trust region (i.e., the initial solution) is used to update the trust region. Additionally, factorization is applied to the subproblem algorithm to enhance both numerical stability and computational efficiency [18,19]. In this study, Cholesky factorization was employed as a commonly used method with the TRR algorithm [9,11].

2.2.4. *Correlation performance sensitivity to empirical coefficient number*

A sensitivity analysis was conducted in the present work to evaluate the predictive performance of the proposed correlations with varying numbers of empirical coefficients. This analysis relied on applying the hold-out technique (also known as the validation set approach) [20], where 85 % of the whole dataset was used for training (i.e., fitting the correlation and estimating the empirical coefficients), while the remaining 15 % was used for testing (i.e., assessing the prediction accuracy on unseen data). In addition, a K-fold cross-validation technique [21] was employed to further assess the robustness of the proposed correlation against over-fitting, examining their stability, consistency of error across folds, and insensitivity to data partitioning [22]. Further details regarding the selection process for the number of coefficients and the compromise between fitting accuracy and number of coefficients with avoiding the risk of overfitting, are provided in Sections (S.4-S.10) in the Supplementary Materials.

3. Results and discussions

An empirical correlation for the K-site LH_2 tank was developed using the TRR optimization algorithm. This correlation provides an analytical formula that relates the final vapor pressure (P_f, in MPa) to five operating variables; namely initial operating pressure (P_i, in MPa), heat flux (q, in W/m^2), initial liquid filling ratio (φ), tank volum (V, in m^3), and hold time (t, in hr), as shown in Eq. (4). The correlation includes 30 unknown coefficients, which were accurately determined using the TRR algorithm. The values of coefficients C_1 to C_{30} are provided in Section S.11 in the Supplementary Materials.

$$P_f = C_{11} \times e^{\left\{ \begin{array}{c} \left(C_1 \times P_i^{C_2}\right) + \left(C_3 \times \varphi^{C_4}\right) + \left(C_5 \times q^{C_6}\right) + \left(C_7 \times V^{C_8}\right) + \left(C_9 \times t^{C_{10}}\right) + \\ \left[C_{12} \times \left(P_i^2\right)^{C_{13}}\right] + \left[C_{14} \times \left(\varphi^2\right)^{C_{15}}\right] + \left[C_{16} \times \left(q^2\right)^{C_{17}}\right] + \left[C_{18} \times \left(V^2\right)^{C_{19}}\right] + \\ \left[C_{20} \times \left(t^2\right)^{C_{21}}\right] + \left[C_{22} \times \left(P_i \times V\right)^{C_{23}}\right] + \left[C_{24} \times \left(\varphi \times V\right)^{C_{25}}\right] + \left[C_{26} \times \left(\varphi \times q\right)^{C_{27}}\right] + \\ \left[C_{28} \times \left(P_i \times t\right)^{C_{29}}\right] \end{array} \right\}} - C_{30} \tag{4}$$

To analyze the proposed empirical correlation for the K-site LH_2 tank, convergence to the lowest *RMSE* was monitored across iterations with various initial guesses for the 30 unknown coefficients, ranging from 0.0001 to 0.1, as shown in Fig. 2(a). The least *RMSE* was achieved with an initial guess of 0.01. Fig. 2(b) illustrates the predictions of final vapor pressure at different initial guesses, demonstrating the significant impact of appropriate initial values on prediction accuracy. It was confirmed that the TRR algorithm yields highly accurate results when proper initial guesses were selected for the coefficients. With an initial guess of 0.01 for all coefficients, the predicted final vapor pressure closely matched experimental data under various operating conditions, as shown in Fig. 3(a).

Furthermore, Fig. 3(b) displays the over- and under-predictions of

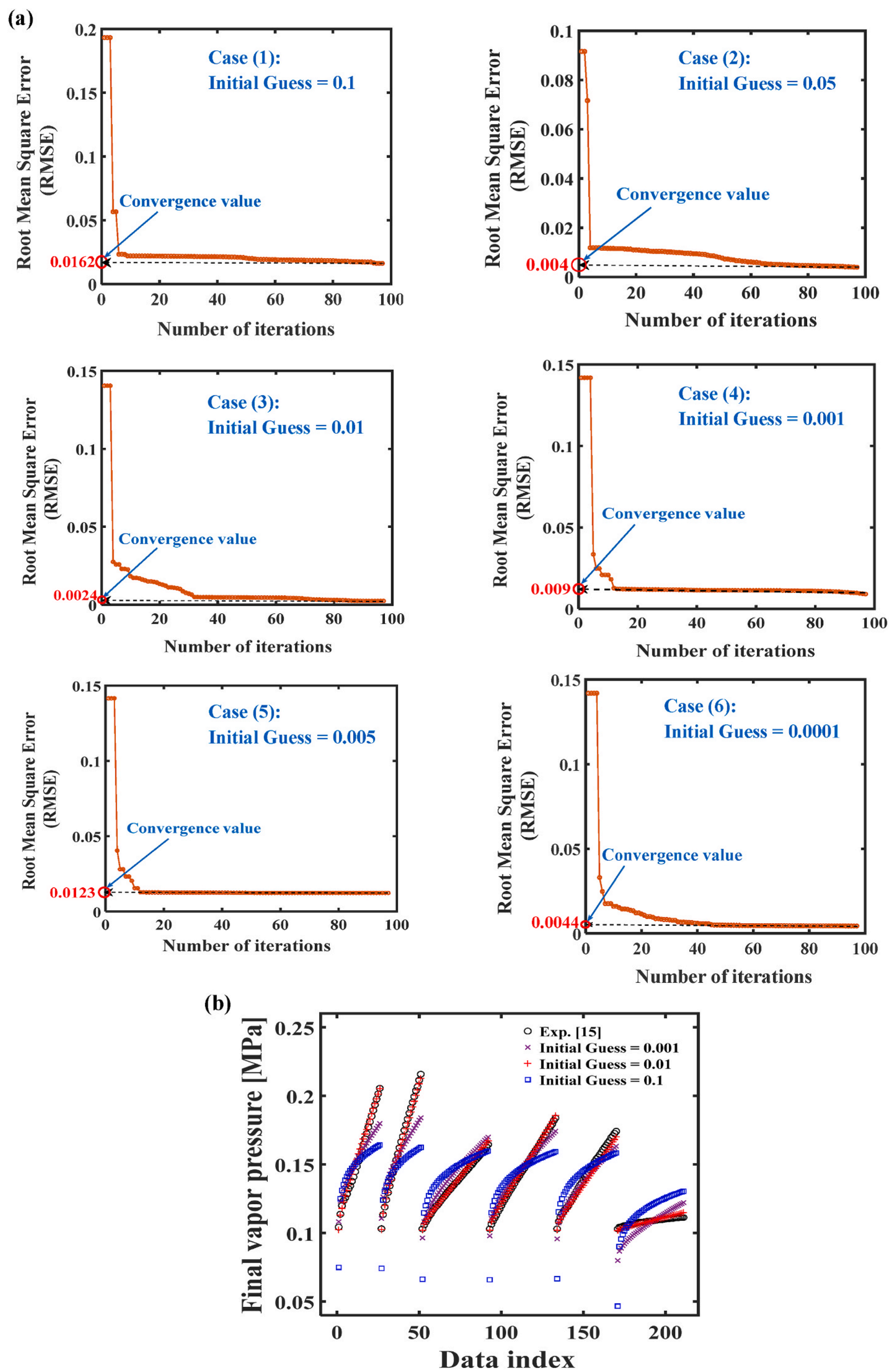

Fig. 2. Development of the proposed empirical correlation for predicting the final vapor pressure in K-site LH_2 tank: (a) Convergence trend of *RMSE* during the iterative optimization process based on the TRR approach; and (b) Predicted *vs.* actual values for the final vapor pressure at different initial guesses.

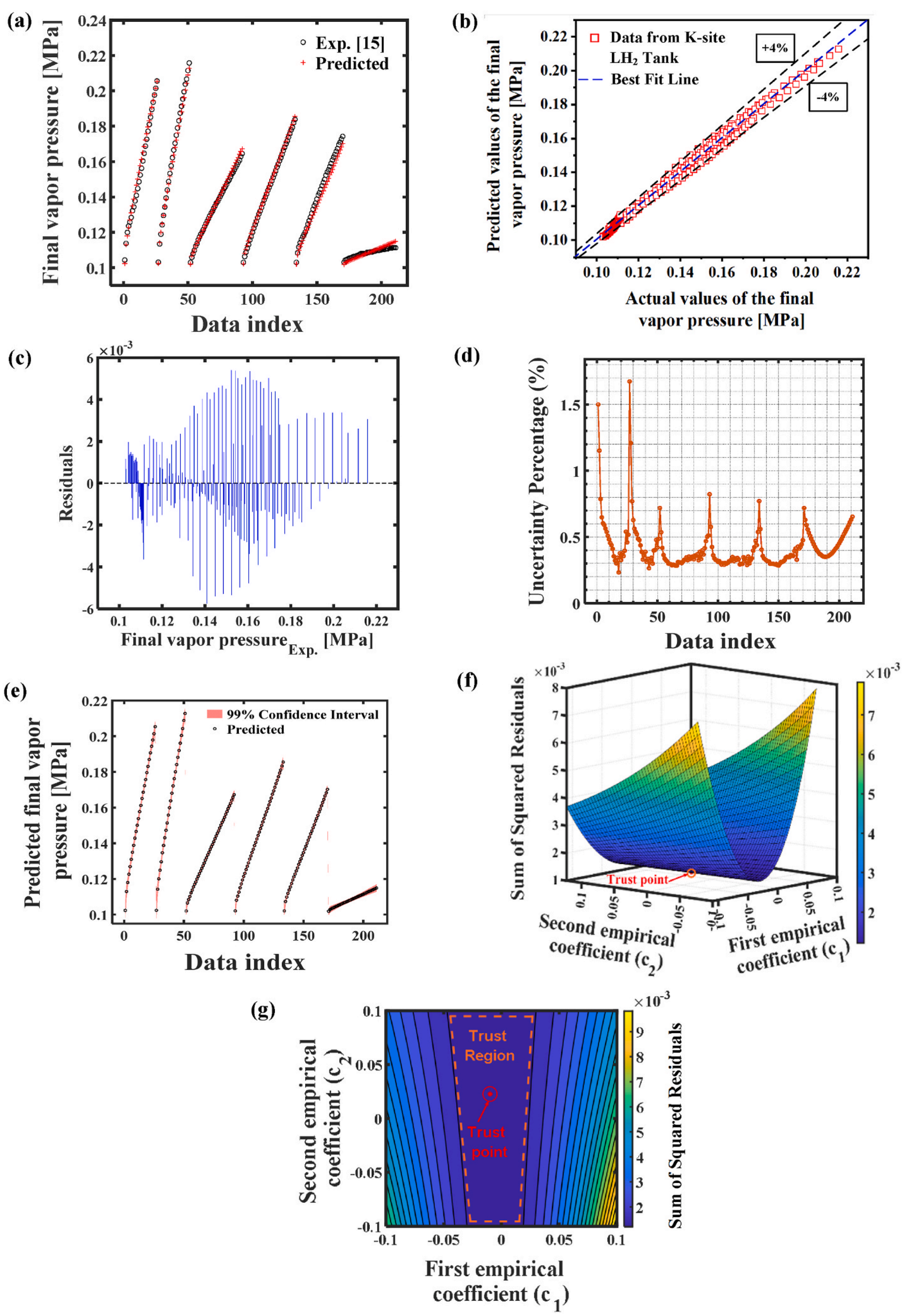

Fig. 3. Performance evaluation for the proposed empirical correlation related with predicting the final vapor pressure in the K-site LH_2 tank: (a, b) Predicted *vs.* experimental values with error analysis; (c) Residuals of the fit; (d) Uncertainty percentage of the predictions; (e) Confidence intervals for the estimated coefficients; and (f, g) Visualization of trust region for a sample of empirical coefficients.

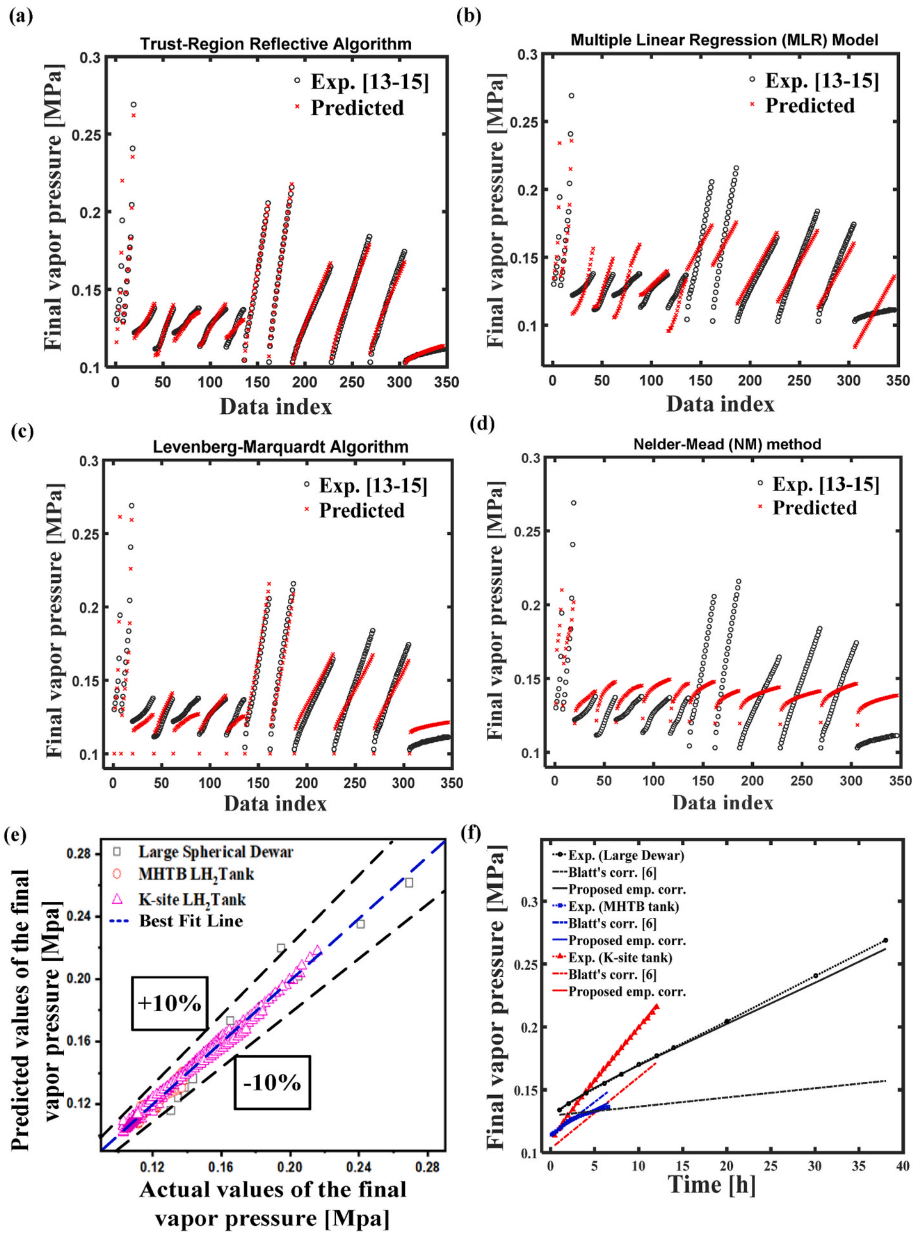

Fig. 4. Assement of the proposed extended empirical correlation: (a–d) Predicted *vs.*experimental results; (e) Error analysis for the predicted results; and (f) General assessment for the proposed extended empirical correlation compared to experimental results and Blatt's empirical correlation predictions [6]. [**For Large Dewar:** $q = 1.9$ W/m^2, $FR = 54.2$ %, $P_{\text{ini}} = 0.129$ MPa; **For MHTB tank:** $q = 2.0518$ W/m^2, $FR = 90$ %, $P_{\text{ini}} = 0.113$ MPa; **For K-site tank:** $q = 3.5$ W/m^2, $FR = 29$ %, $P_{\text{ini}} = 0.103$ MPa].

the final vapor pressure, with an acceptable error margin of $\pm$ 4% and an average prediction error of 1.3 %, demonstrating the reliability of the proposed empirical correlation. Meanwhile, Fig. 3(c) shows the fit residuals where fluctuations in the residuals are expected in empirical modeling. Such fluctuations arise from natural variability in the predicted data, which includes minor prediction uncertainties. From Fig. 3 (c), it can be noticed that these fluctuations are almost distributed symmetrically around zero residual line, validating the reliability of the K-site empirical correlation with unbiased scatter. On the other hand, Fig. 3(d) presents the uncertainty percentages, indicating low uncertainty and highlighting the accuracy of the predictions with minimal deviation from the true values. Also, statistical confidence assessment was further conducted to estimate the confidence intervals around the predicted values, revealing that the estimated coefficients are likely to fall within a 99 % confidence interval, as shown in Fig. 3(e). This demonstrates the high accuracy of the proposed empirical correlation from a practical perspective. Also, Fig. 3(f) and (g) illustrate the trust region for a sample of empirical coefficients where the Sum of Squared Residuals (*SSR*) is minimized.

After confirming the effectiveness of the TRR approach in developing an accurate empirical correlation for self-pressurization in the K-site LH_2 tank, it is applied to derive an extended empirical correlation for the three considered LH_2 tanks, including the MHTB [13], the large spherical Dewar [14], and the K-site tank [15]. This correlation is extensively developed by combining experimental data from these three LH_2 tanks, under the same design parameters. Building on the analytical formula for the K-site LH_2 tank presented in Eq. (4), this formula was extended by adding additional coefficients and incorporating polynomial effects, including variable interactions within the exponential function. Given the relationship between final vapor pressure and hold time [2], an exponential function with 64 empirical coefficients is proposed, as shown in Eq. (5), to develop the extended empirical correlation. The values of coefficients C_1 to C_{64} are provided in Section S.12 in the Supplementary Materials.

$$P_f = C_{11} \times e^{\left\{\begin{array}{c} \left(C_1 \times P_i^{C_2}\right)+\left(C_3 \times \varphi^{C_4}\right)+\left(C_5 \times q^{C_6}\right)+\left(C_7 \times V^{C_8}\right)+\left(C_9 \times t^{C_{10}}\right)+ \\ \left[C_{12} \times \left(P_i^2\right)^{C_{13}}\right]+\left[C_{14} \times \left(\varphi^2\right)^{C_{15}}\right]+\left[C_{16} \times \left(q^2\right)^{C_{17}}\right]+\left[C_{18} \times \left(V^2\right)^{C_{19}}\right]+ \\ \left[C_{20} \times \left(t^2\right)^{C_{21}}\right]+\left[C_{22} \times (P_i \times V)^{C_{23}}\right]+\left[C_{24} \times (\varphi \times V)^{C_{25}}\right]+\left[C_{26} \times (\varphi \times q)^{C_{27}}\right]+ \\ \left[C_{28} \times (P_i \times t)^{C_{29}}\right]+\left[C_{31} \times (P_i \times \varphi)^{C_{32}}\right]+\left[C_{33} \times (\varphi \times t)^{C_{34}}\right]++\left[C_{35} \times (q \times V)^{C_{36}}\right]+ \\ \left[C_{37} \times (q \times t)^{C_{38}}\right]+\left[C_{39} \times \left(P_i^2 \times \varphi\right)^{C_{40}}\right]+\left[C_{41} \times \left(P_i^2 \times V\right)^{C_{42}}\right]+\left[C_{43} \times \left(P_i^2 \times t\right)^{C_{44}}\right]+ \\ \left[C_{45} \times \left(\varphi^2 \times q\right)^{C_{46}}\right]+\left[C_{47} \times \left(\varphi^2 \times V\right)^{C_{48}}\right]+\left[C_{49} \times \left(\varphi^2 \times t\right)^{C_{50}}\right]+\left[C_{51} \times \left(q^2 \times V\right)^{C_{52}}\right]+ \\ \left[C_{53} \times \left(q^2 \times t\right)^{C_{54}}\right]+\left[C_{55} \times \left(P_i^3\right)^{C_{56}}\right]+\left[C_{57} \times \left(\varphi^3\right)^{C_{58}}\right]+\left[C_{59} \times \left(q^3\right)^{C_{60}}\right]+ \\ \left[C_{61} \times \left(V^3\right)^{C_{62}}\right]+\left[C_{63} \times \left(t^3\right)^{C_{64}}\right] \end{array}\right\}} + C_{30} \tag{5}$$

under the same dataset. This indicates that while the extended correlation generalizes well across different LH_2 tank configurations, it retains the same level of accuracy for the K-site tank. Therefore, the 64-coefficient extended correlation offers broader applicability without compromising prediction accuracy for individual configurations like the K-site LH_2 tank. A complete comparison between both correlations with calculations, has been provided in Section S.15 in the Supplementary Materials. These findings underscore the strong predictive capability of the proposed extended empirical correlation for self-pressurization under various design conditions.

On the other hand, the prediction performance of the proposed extended empirical correlation is illustrated in Fig. 4. In more detail, for the sake of general assessment and comparison, and verifying the attractiveness of using the Trust-Region Reflective (TRR) algorithm in the present study, other linear/nonlinear parameter fitting approaches, including Multiple Linear Regression (MLR) [23], Levenberg-Marquardt (LM) [24], and Nelder-Mead (NM) [25] methods, were applied to the investigated problem. The prediction performances of the considered four algorithms are illustrated in Fig. 4(a–d). From such a figure, it can be noticed that the TRR algorithm outperformed the other investigated parameter fitting methods, enhancing the strength and practical relevance of this study. Further details on the MLR, LM, and NM methods are provided in Sections S.13 and S.14 in the Supplementary Materials. Table 3 illustrates the prediction error percentages during training and testing phases for evaluating the robustness of the extended developed empirical correlation under different parameter fitting methods. From such a table, it can be noticed the superiority of the TRR algorithm over its counterparts with the least average prediction errors during training and testing phases (i.e., highest predictive capability).

As shown in Fig. 4(a), the predicted results closely align with the experimental data, indicating a high degree of agreement. Meanwhile, error analysis in Fig. 4(e) reveals that most of the predictions fall within an acceptable error margin of $\pm$ 10%, with an average prediction error of 1.49 %, emphasizing the robustness of the proposed extended empirical correlation. To further validate the applicability of the proposed extended correlation, a comparative analysis was conducted against Blatt's empirical correlation [6], as shown in Fig. 4(f). The results indicate that the proposed correlation aligns closely with experimental data, while Blatt's correlation [6] exhibits significant discrepancies. These discrepancies are attributed to several factors: (i) the assumption of a linear relationship between final vapor pressure and hold time; (ii) the insufficiency of experimental LH_2 data used to develop Blatt's correlation; (iii) the limitations in geometrical and operational ranges, leading to inaccuracies outside the specified range; and (iv) the inability to capture interactions between variables affecting pressure evolution due to the limited number of LH_2 experimental data. These limitations undermine the reliability of Blatt's empirical correlation. In contrast, the proposed extended correlation accounts for these factors, yielding more accurate predictions, as demonstrated in Fig. 4(f).

To further validate its predictability, the proposed extended 64-coefficient correlation has been tested on the K-site LH_2 data to demonstrate whether it improves the prediction accuracy of the 30-coefficient correlation or not. It was found that the proposed 64-coefficient correlation has achieved the same prediction accuracy (i.e., average prediction error) attained by the 30-coefficient correlation. Specifically, the extended 64-coefficient correlation yielded an average error of 1.3 %, which is the same as that achieved by the 30-coefficient correlation

4. Conclusions

A developed empirical correlation for self-pressurization in multi-configuration LH_2 tanks has been presented using the trust-region reflective (TRR) optimization algorithm. This correlation predicts final vapor pressure as a response to five key design parameters, namely initial operating pressure, heat flux, initial liquid filling ratio, tank volume, and hold time. It demonstrates strong applicability across various LH_2 tank sizes, shapes and operational ranges. Specifically, the initial operating pressure ranges from 0.1 to 0.13 MPa, heat flux from 0.35 to 3.5 W/m^2, the initial liquid filling ratio from 25 % to 90 %, and tank volume from 4.89 to 208 m^3. Compared to experimental results, the correlation's predictions fall within an acceptable error margin of $\pm$ 10%, with an average error of 1.49 %. This underscores the robustness and superior accuracy of the proposed empirical correlation over existing correlations. Furthermore, the predicted results closely align with the experimental data, capturing both the trend and behavior.

The TRR algorithm has proven to be a robust optimization method for nonlinear parametric fitting. Future research will focus on integrating the developed empirical correlation with relevant theoretical models to create a more comprehensive predictive framework. Moreover, combining the developed correlation with dynamic control systems will be explored to control pressure buildup and mitigate venting risks. Other design optimization techniques, such as swarm meta-heuristic algorithms, will also be considered in future work. This work provides valuable insights and practical guidance for the design of multi-scale LH_2 tanks and paves the way for further application of nonlinear parametric fitting approaches in the LH_2 research field.

CRediT authorship contribution statement

Anas A. Rahman: Writing – original draft, Visualization, Validation, Software, Methodology, Investigation, Formal analysis, Data curation, Conceptualization. **Bo Wang:** Writing – review & editing, Visualization, Supervision, Resources, Funding acquisition. **Jingshan Yan:** Writing – review & editing, Investigation. **Haoren Wang:** Writing – review & editing, Investigation. **Tao Jin:** Writing – review & editing, Supervision. **Zhihua Gan:** Writing – review & editing, Supervision, Funding acquisition.

Declaration of competing interest

The authors declare that they have no known competing financial interests or personal relationships that could have appeared to influence the work reported in this paper.

Acknowledgment

This research was supported by the National Natural Science Foundation of China under Grant No. 52476020 and the Baima Lake Laboratory Joint Funds of the Zhejiang Provincial Natural Science Foundation of China under Grant No. LBMHZ24E060004.

Appendix A. Supplementary data

Supplementary data to this article can be found online at https://doi.org/10.1016/j.ijhydene.2025.05.393.

References

[1] Wang H, Wang B, Sun J, Pan Q, Luo G, Tao X, He Y, Pfotenhauer J, Jin T, Gan Z. Experimental and computational fluid dynamic investigation on thermal behaviors of liquid hydrogen during the no-vented storage process: a literature review. Int J Hydrogen Energy 2024;57:822–43.
[2] Rahman AA, Wang H, Wang B, Xu T, Li J, He Y, Jin T, Gan Z. Prediction of pressure evolution in non-venting self-pressurized liquid hydrogen tanks using artificial neural network approach. Int J Hydrogen Energy 2024;68:428–39.
[3] Wang Z, Mérida W. Thermal performance of cylindrical and spherical liquid hydrogen tanks. Int J Hydrogen Energy 2024;53:667–83.
[4] Rotenberg Y. Numerical simulation of self-pressurization in a small cryogenic tank. Adv Cryog Eng 1986;29:963–71.
[5] Агафоноϑ и M, доMa♯енко AM. Liquid cryogenic system. Translated by ZHAO yunsheng & CUI yune. Beijing: Cryogenics Editorial Office; 1993. p. 37–8 (in Chinese).
[6] Blatt MH. Empirical correlations for pressure rise in closed cryogenic containers. J Spacecraft Rockets 1968;5(6):733–5.
[7] Yuan YX. Recent advances in trust region algorithms. Math Program 2015;151: 249–81.
[8] Wu L, Chen Z, Long C, Cheng S, Lin P, Chen Y, Chen H. Parameter extraction of photovoltaic models from measured IV characteristics curves using a hybrid trust-region reflective algorithm. Appl Energy 2018;232:36–53.
[9] Conn AR, Gould NI, Toint PL. Trust region methods. first ed. Philadelphia, PA: Society for Industrial and Applied Mathematics Press; 2000.
[10] Le TM, Fatahi B, Khabbaz H, Sun W. Numerical optimization applying trust-region reflective least squares algorithm with constraints to optimize the non-linear creep parameters of soft soil. Appl Math Model 2017;41:236–56.
[11] Gao X, Hou Q, Yao S, Zhou K. Opposite normalized trust-region reflective (ONTRR): a new algorithm for parameter extraction of single, double and triple diode solar cell models. Appl Sci 2023;13(14):8199.
[12] Rahman AA, Wang B, Ji RY, Wang HR, Xu TC, He YX, Jin T, Gan ZH. ANN-Based correlation for predicting self-pressurization rate in quasi-spherical liquid hydrogen storage tanks. Int J Hydrogen Energy 2025;113:614–28.
[13] Hastings LJ, Flachbart RH, Martin JJ, Hedayat A, Fazah M, Lak T, Nguyen H, Bailey JW. Spray bar zero-gravity vent system for on orbit liquid hydrogen storage. NASA TM-12926. 2003. p. 43–133.
[14] Liebenberg DH, Edeskuty FJ. Pressurization analysis of a large-scale liquid-hydrogen dewar. International Advances in Cryogenic Engineering 1965;142(10): 284–9.
[15] Hasan M, Lin CS. Self-pressurization of a flight weight liquid hydrogen storage tank subjected to low heat flux. NASA TM-103804. 1991. p. 2–5.
[16] Coleman TF, Li Y. An interior trust region approach for nonlinear minimization subject to bounds. SIAM J Optim 1994;6(2):418–45.
[17] Coleman TF, Li Y. A reflective Newton method for minimizing a quadratic function subject to bounds on some of the variables. Cornell University; 1992. p. 1040–58.
[18] Branch MA, Coleman TF, Li Y. A subspace, interior, and conjugate gradient method for large-scale bound-constrained minimization problems. SIAM J Sci Comput 1999;21(1):1–23.
[19] Avery P. Applied fitting theory I: general least squares theory. CLEO Note CBX 1991;18:91–172.
[20] James G, Witten D, Hastie T, Tibshirani R. An introduction to statistical learning. first ed. New York: Springer Press.
[21] Krstajic D, Buturovic LJ, Leahy DE, Thomas S. Cross-validation pitfalls when selecting and assessing regression and classification models. J Cheminf 2014;6: 1–15.
[22] Hastie T, Tibshirani R, Friedman J. The elements of statistical learning. second ed. Stanford, CA: Springer Press; 2009.
[23] Chou JS, Chiu CK, Farfoura M, Al-Taharwa I. Optimizing the prediction accuracy of concrete compressive strength based on a comparison of data-mining techniques. J Comput Civ Eng 2011;25(3):242–53.
[24] Gavin HP. The Levenberg-Marquardt algorithm for nonlinear least squares curve-fitting problemsvol. 3. Department of Civil and Environmental Engineering Duke University; 2019. p. 1–23.
[25] Wang PC, Shoup TE. Parameter sensitivity study of the Nelder-Mead simplex method. Adv Eng Software 2011;42:529–33.